JOURNAL OF GEOPHYSICAL RESEARCH, VOL. 114, A01301, doi:10.1029/2008JA013564, 2009

Planetary-scale variability in the low-latitude *E* region field-aligned irregularities: First results from Gadanki observations

D. V. Phanikumar,[1] A. K. Patra,[1] M. V. Ratnam,[1] and S. Sripathi[2]

Received 2 July 2008; revised 3 November 2008; accepted 21 November 2008; published 8 January 2009.

[1] In this paper, we present for the first time planetary-scale wave signatures in the low-latitude *E* region field-aligned irregularities (FAI) observed during June 2004 to May 2005 using the Gadanki mesosphere-stratosphere-troposphere radar. We have observed a clear signature of 5–8 day variability in echo occurrence, in SNR, and also in Doppler velocity observed above 100 km. Concurrent temperature observations made using the Sounding of the Atmosphere using Broadband Emission Radiometry (SABER) on board the Thermosphere-Ionosphere-Mesosphere Energetic and Dynamics (TIMED) satellite have also clearly shown the presence of 5–8 day variability similar to that of FAI. The temperature variations have been characterized with zonal wave numbers of 3 and 4 and vertical wavelength of 15–20 km. These waves are found to have increasing amplitude with increasing height and phase progressing downward, suggesting that they were of lower atmospheric origin. It is emphasized that the planetary-scale characteristics of neutral atmosphere in the FAI observations are important in understanding the vertical coupling of the low-latitude ionosphere-atmosphere system. These observations and the pertinent issues are discussed in the light of current understanding of the planetary-scale role on the FAI variability.

Citation: Phanikumar, D. V., A. K. Patra, M. V. Ratnam, and S. Sripathi (2009), Planetary-scale variability in the low-latitude *E* region field-aligned irregularities: First results from Gadanki observations, *J. Geophys. Res.*, *114*, A01301, doi:10.1029/2008JA013564.

1. Introduction

[2] Low-latitude *E* region irregularities found outside the equatorial electrojet belt (±3° magnetic latitude) appear to be a hybrid of midlatitude and electrojet irregularities [*Chau et al.*, 2002; *Patra et al.*, 2004]. They show quasiperiodic (QP) echo occurrence [*Choudhary and Mahajan*, 1999; *Chau and Woodman*, 1999; *Venkateswara Rao et al.*, 2008] and spectral features [*Krishna Murthy et al.*, 1998; *Woodman et al.*, 1999] similar to those of midlatitudes [*Yamamoto et al.*, 1991], but are also found during midday hours like those of electrojet [*Patra et al.*, 2004].

[3] The descending echoing layers and the quasiperiodic occurrence of the echoes from the low-latitude *E* region irregularities have been attributed to the effects of neutral wind and wind shear [*Patra et al.*, 2002, 2006, 2007; *Sripathi et al.*, 2003; *Choudhary et al.*, 2005]. We have extended the low-latitude observations and found planetary-scale wave signatures of the neutral atmosphere in the data. Considering that the low-latitude *E* region is connected to the equatorial *F* region through the magnetic field lines, low-latitude plasma irregularities having a link with neutral winds of different scales should be considered important in a wider perspective to the equatorial aeronomy. For example, the day-to-day variability in the equatorial spread *F* occurrence continues to be a puzzle and in this regard, any variability in the low-latitude *E* region plasma instability processes might play an important role.

[4] At present there are two reports from midlatitude investigations on *E* region echo occurrence and sporadic *E* (E_s) that show the signature of planetary-scale waves. The first one, made by *Tsunoda et al.* [1998], showed that the occurrence of midlatitude QP echoes have a 5 days periodicity. *Voiculescu et al.* [1999] showed that the occurrences in midlatitude radar backscatter and sporadic *E* (E_s) top frequency have a clear signature of planetary-scale waves with a 2–9 day period that strengthened the foundation of the planetary waves playing a role on the *E* region plasma structures and irregularities.

[5] The presence of planetary-scale variations in wind [*Wu et al.*, 1994] and electron density in the ionosphere was known earlier [*Fraser*, 1977; *Chen*, 1992; *Pancheva et al.*, 1991; *Lastovicka et al.*, 1994; *Apostolov et al.*, 1995], but similar variations in E_s or small-scale irregularities were not known. Thus, the observations made by *Tsunoda et al.* [1998] and *Voiculescu et al.* [1999] opened up a new dimension to the investigations on the long-term variability of E_s and small-scale irregularities in the midlatitude *E* region.

[6] Soon after the first observations of planetary-scale variability in E_s and FAI, two mechanisms, to account for the observations were proposed: (1) a planetary-scale wind-driven dynamo electric field varying with the same planetary scale modulates the *E* region irregularity generation [*Tsunoda et al.*, 1998] and (2) planetary-scale winds form plasma structures through ion convergence, and the en-

[1]National Atmospheric Research Laboratory, Gadanki, India.
[2]Indian Institute of Geomagnetism, Navi Mumbai, India.

0148-0227/09/2008JA013564$09.00

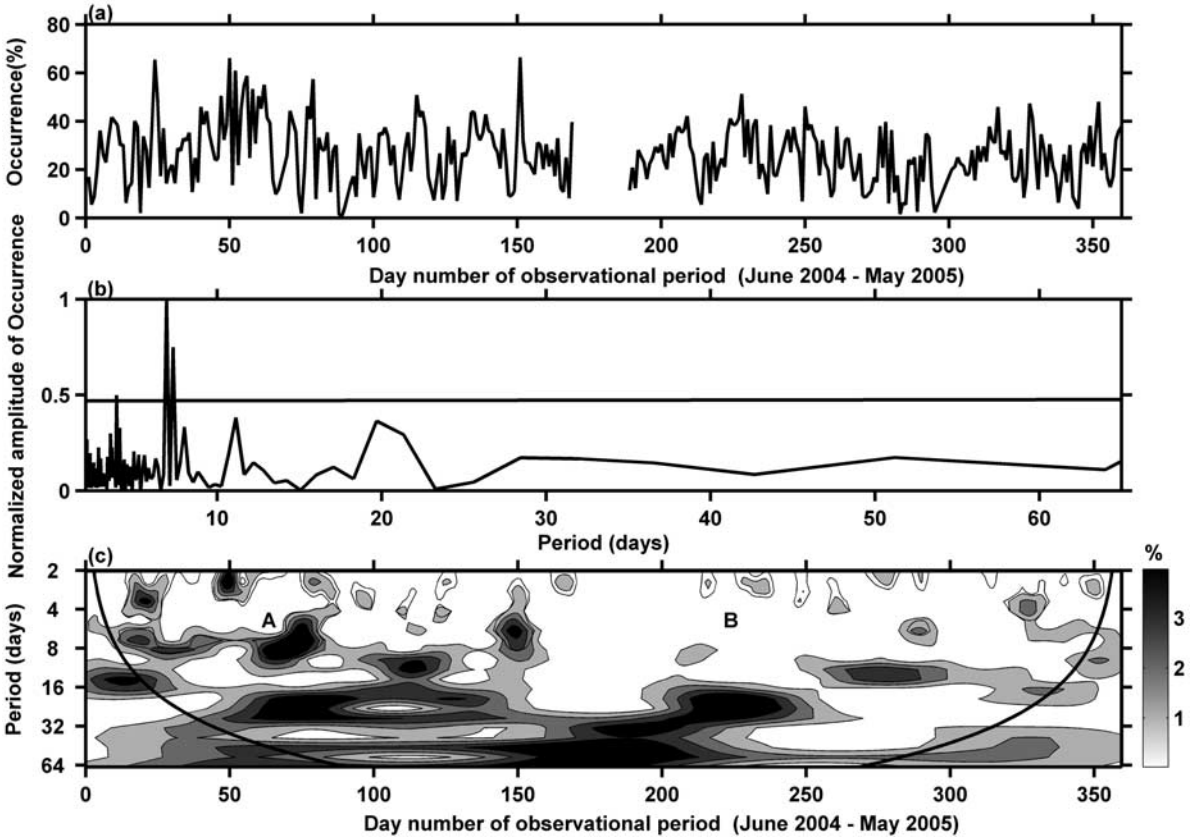

Figure 1. (a) Time series of radar echo occurrence of *E* region FAI observed during the period of June 2004 to May 2005, (b) normalized amplitudes of radar echo occurrence for different periods, and (c) dominant periods as a function of day number. The horizontal line in Figure 1b represents the 99% confidence level. The solid line in Figure 1c represents the cone of influence, and "A" and "B" represent two periods selected for further analysis.

hanced plasma structures turn unstable, generating irregularities [*Shalimov et al.*, 1999]. A number of observational and theoretical studies on the role of planetary-scale waves modulating the midlatitude E_s have since been carried out [*Voiculescu et al.*, 2000; *Igarashi and Kato*, 2001; *Haldoupis and Pancheva*, 2002; *Shalimov and Haldoupis*, 2002; *Voiculescu and Ignat*, 2003; *Pancheva et al.*, 2003; *Haldoupis et al.*, 2004]. While these studies have made significant progress in both observations and physical understanding, much is yet to be learned on the true role of the planetary-scale waves that is now presumed to control the *E* region plasma structures and small-scale irregularities.

[7] Considering that the planetary-scale waves are global in nature and that their role could also be seen in the low-latitude *E* region plasma irregularities, we have conducted experiments using the Gadanki mesosphere-stratosphere-troposphere (MST) radar covering all seasons. In this paper, we present and discuss a few days variability observed in the low-latitude *E* region irregularities. We present global temperature data provided by the Sounding of the Atmosphere using Broadband Emission Radiometry (SABER) on board the Thermosphere-Ionosphere-Mesosphere Energetic and Dynamics (TIMED) satellite to evaluate the observed variabilities in terms of planetary-scale waves. The study presented here is the first of its kind from Gadanki and also from the low-latitude region, and is significant in understanding the role of planetary-scale waves in the *E* region plasma irregularities in general.

2. A Brief Description of the Observations and Data

2.1. MST Radar Observations

[8] Observations used for the analysis were made using the MST radar located at Gadanki (13.5°N, 79.2°E, magnetic latitude 6.4°) [*Rao et al.*, 1995].This radar is a high-power coherent pulsed Doppler radar operating at 53 MHz with a maximum peak power of 2.5 MW and antenna aperture of 130 × 130 m^2. The antenna array consists of 32 × 32 three-element Yagi antennas, which generates a radiation pattern with main lobe of 2.8° (one way 3 dB full width), gain of 36 dB, and first side lobe level of −20 dB at 4° from the main lobe. The horizontal dimension of the 2.8° wide beam at 100 km altitude is 4.9 km. For the *E* region FAI studies from Gadanki, the antenna beam is tilted at 13° off zenith due north, which satisfies perpendicularity to the Earth's magnetic field, for the reception of the coherent backscattered echoes. To study planetary-scale wave activity of low-latitude *E* region FAI, we conducted experiments at intervals of 6 h (i.e., 0000, 0600, 1200 and 1800 LT) from June 2004 to May 2005, and collected 40 sets of height profile of power spectrum on every occasion. The observa-

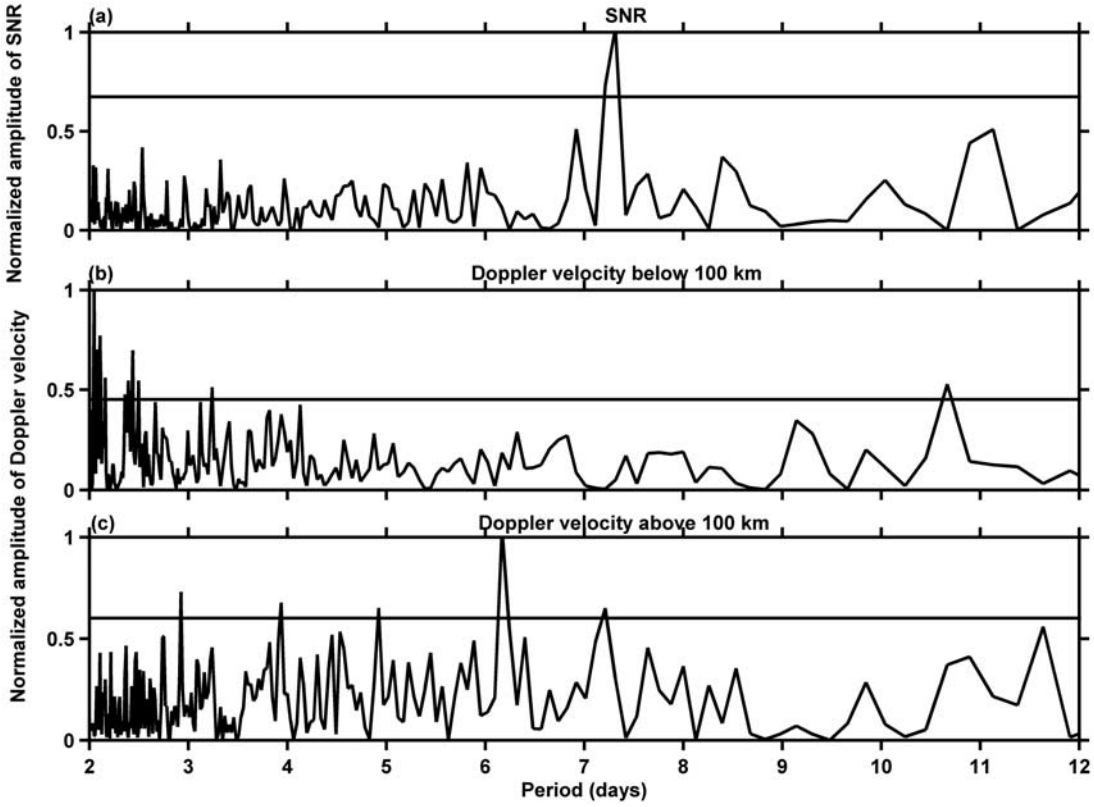

Figure 2. Normalized amplitudes for different periods in (a) SNR, (b) the Doppler velocity observed below 100 km, and (c) the Doppler velocity observed above 100 km during the period June 2004 to May 2005. The horizontal line represents the 99% confidence level.

tions were made using an uncoded pulse of 8 μs width with interpulse period of 2000 μs. We performed 2 coherent integrations and collected 256 samples for performing FFT to construct power spectrum. Then, 8 such spectra were averaged and the resultant spectra were stored for off-line data processing. With these, we obtained observations with a range resolution of 1.2 km, an unambiguous Doppler velocity window of ±353.75 m s^{-1}, and a velocity resolution of 2.76 m s^{-1}. Power spectrum data were processed off-line to obtain SNR, mean Doppler, and spectral width. SNRs, used in the present study, were computed using noise power reckoned over the entire observational Doppler window of ±353.75 m s^{-1}. No sky noise correction or calibration has been made. We find that the maximum SNR is 30 dB and all signals with SNR > −5 dB (which are 5 dB larger than noisy signals) can be reliably used for scientific investigations.

[9] Echo occurrence, SNR, and Doppler velocity used in the present study correspond to signals having SNR > −5 dB; and the height region considered is 90.6–109.8 km. Echo occurrence rate S (%) used here is height invariant and has been calculated as

$$S = \left(\frac{\sum m_i}{\sum n_i}\right) \times 100, \quad (1)$$

where m is the number of range bins where signals exceed SNR > −5 dB, n is the total number of range bins in the height region of 90.6–109.8 km (i.e.,16 range bins), and i is the number of scan cycles (i.e., 40). Then the average occurrence rate of echoes per day (averaged for four time durations) has been calculated. In the case of Doppler velocity, the height region has been divided into two regions: one below 97 km (90.6–96.6 km) and another above 100 km (100.2–109.8 km). We consider that velocities observed below 97 km would be controlled by the neutral wind, whereas velocities observed above 100 km would be controlled by the electric field because of the decreasing value of collision frequency with height [*Krishna Murthy et al.*, 1998].

2.2. Global Measurements of Temperature From SABER

[10] In order to study planetary-scale activities, we have used temperature data, concurrent to radar observations of FAI, obtained with the SABER. The instrument performs an up/down scan of the Earth's horizon once every 58 s for making measurements of temperature and various constituents. It measures optical radiations from limb direction in 10 broadband spectral channels ranging from 1.27 μm to 17 μm. The kinetic temperature from tropopause to lower thermosphere is retrieved from CO_2 15 μm emission using a full nonlocal thermal equilibrium (LTE) inversion [*Mertens et al.*, 2001]. During daytime, the required CO_2 concentration is retrieved from the SABER observation itself, whereas during nighttime it was taken from the

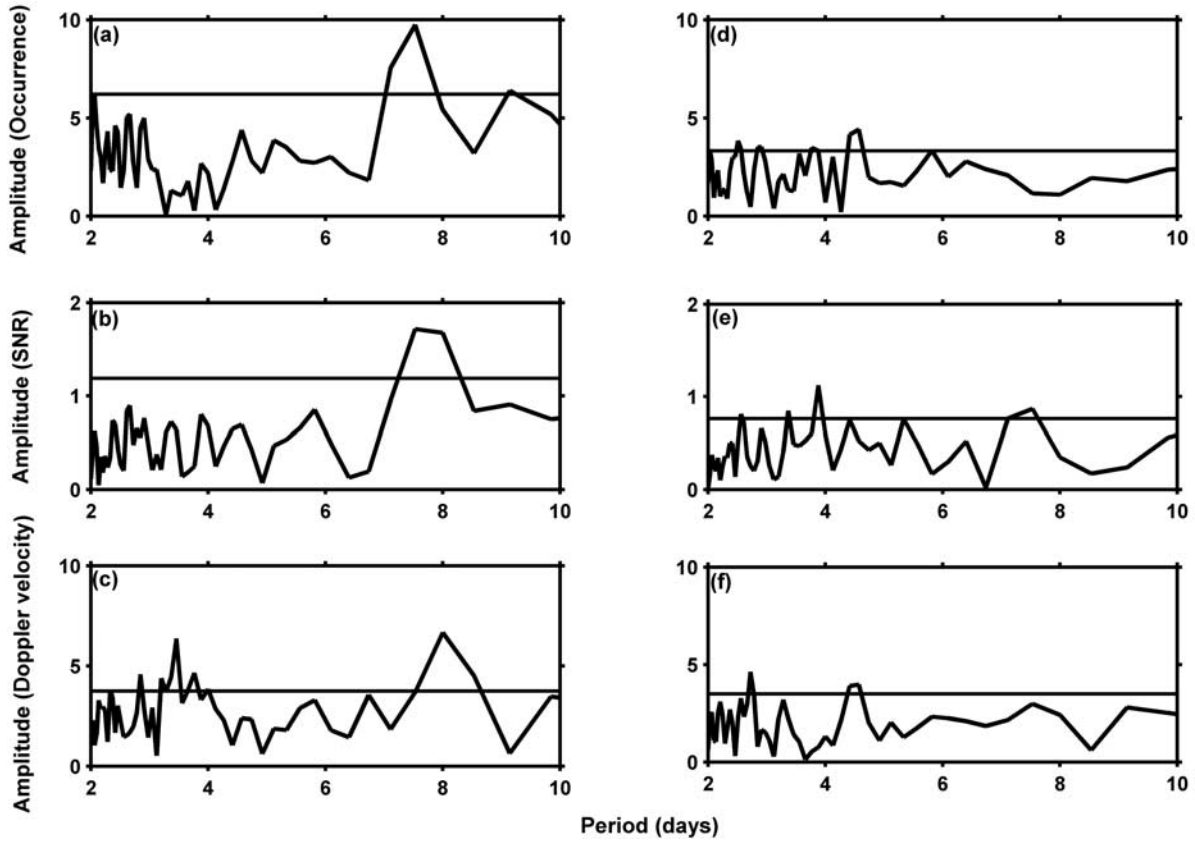

Figure 3. Normalized amplitude for different periods observed in radar echo occurrence, SNR, and Doppler velocity during (a–c) July–August 2004 and (d–f) January–February 2005, respectively. The horizontal line in each plot represents the 99% confidence level.

TIME-GCM (Thermosphere, Ionosphere, Mesosphere and Electrodynamics General Circulation Model) climatology. *Mertens et al.* [2001] calculated the retrieval uncertainty and found that the uncertainty increases from 1.4 K at 80 km to 4 K at 100 km. The spacecraft was stabilized in a highly inclined orbit (74°) and it can provide data covering 24 h local time over a period of 60 days (for details, see *Xu et al.* [2007]). It is convenient to study the long-period/long-wavelength waves with global temperature data as it provides ~1350 profiles per day over the entire globe. The present study uses Version 1.06 Level 2A data, which is publicly available and is distributed through the SABER team's web site (www.saber.larc.nasa.gov). The height resolution of the temperature data is 2 km.

3. Results

3.1. Variabilities in the *E* Region FAI Observations

[11] Figure 1a shows variation in the echo occurrence (in percent) as a function of the day for the observations made during June 2004 to May 2005. Figure 1b shows normalized amplitude of occurrence with periods between 2 and 60 days. For this computation, the data gap is filled with cubic spline fitted values. Dominant periodicities of 3–4, 5–8 and 10–12 days in the echo occurrence can be noticed. Other periods that are detectable but less significant are 18–22 and 40–60 days. The most significant periodicities (above 99% confidence level), however, occur in a broad range of 5–8 days. Figure 1c shows dominant periods as a function of day number obtained through wavelet analysis. As can be noticed the 5–8 day wave is dominant in the first half of the observational period. We have chosen the observational periods of July–August 2004, marked as "A", when the amplitude of the 5–8 day wave is the strongest; and January–February 2005, marked as "B", when nearly no 5–8 day wave activity exists, for further analysis. These periods fall in the local summer and winter, respectively.

[12] We also looked for these periods in SNR and Doppler velocities of the echoes. Figures 2a–2c show the normalized amplitudes of different periods in the average SNR, in the Doppler velocity observed below 97 km altitude, and in the Doppler velocity observed above 100 km altitude, respectively. It may be mentioned that for the north bearing of the Gadanki radar, the Doppler velocities observed below 97 km represent meridional neutral wind. Similarly, Doppler velocities observed above 100 km represent electrodynamical drift due to the zonal electric field. Figures 2a and 2c clearly show periodicity of 5–8 days in both the average SNR and Doppler velocities observed above 100 km. Doppler velocities observed below 97 km, however, do not show such periodicity. This result is understandable considering that the velocity observed below 97 km is governed by the meridional neutral wind in

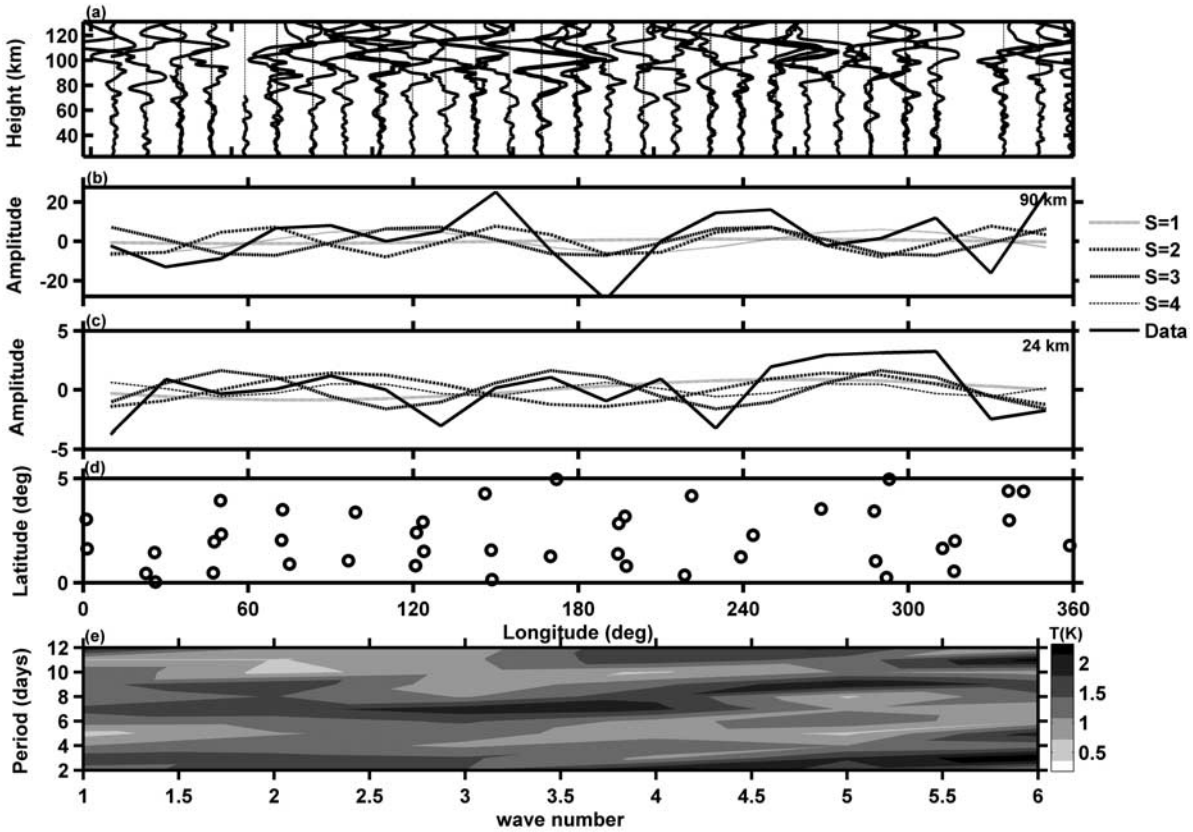

Figure 4. (a) Profiles of temperature fluctuation (T') over 10°N–10°S latitude, longitudinal variations of T' (thick lines), and the fitted T' for wave numbers 1–4 (dotted lines) at an altitude of (b) 90 and (c) 24 km observed on 6 July 2004. Each T' profile (curve) in Figure 4a is plotted at its corresponding longitude (dotted line), where 1 K is equivalent to 3° in longitude. (d) Locations of SABER events on 6 July 2004. (e) Space-time spectral analysis of temperature observations from SABER carried out at 90 km altitude during July–August 2004.

which planetary-scale wave dynamics are not expected to be significant for the low latitude of Gadanki, since the dominant amplitude of planetary-scale wave-related wind would be in the zonal direction [*Wu et al.*, 1994].

[13] Observations made during July–August 2004 and January–February 2005, which are contrasting in nature, are analyzed further and the results are presented in Figures 3a–3c and 3d–3f, respectively. A 5–8 day wave is clearly seen in all the parameters in July–August, but not observed in January–February. Although, other wave periods are also visible in some parameters, we concentrate here only on the dominant periods of 5–8 days. In order to evaluate the contrasting behavior of planetary-scale variability in July–August and January–February and their relationship related to planetary-scale waves we evaluate by temperature observations whether similar contrasting features are present in the two seasons, in the following.

3.2. The 5–8 Day Waves in SABER Temperature

[14] In order to examine the 5–8 day wave activities observed in temperature and compare them with the FAI observations, we have used temperature data corresponding to July–August 2004 and January–February 2005. The SABER temperature data at each height are initially divided into their symmetric and antisymmetric components with respect to the equator. The raw temperature data are binned into ±10° about the equator with temporal resolution of 1 day and longitude width of 30°. Daily binning of the data provides adequate time resolution to study the 5–8 day wave but averaging the temperature perturbations over this longitude and latitude range degrades the spatial resolution by changing the exact SABER profile's coordinates to that of the average bin coordinates. This adds some noise to low wave number waves and attenuates the signal of higher wave number waves. Data are used where there are at least five profiles in a cell. Any grid cells with fewer profiles are linearly interpolated across. Observations corresponding to the height region of 20–110 km with height resolution of 2 km have been used for the analysis. The zonal mean daily temperature is removed from individual temperature measurement made at each height and for each day to get temperature fluctuation. These temperature fluctuations in each grid cell are then averaged to get a mean profile of temperature fluctuations (T'). Fourier analysis is performed on these T' using a nonoverlapping 31 day time window. Waves are extracted using space-time spectral analysis separately on the symmetric and antisymmetric components. This analysis is appropriate for data which are

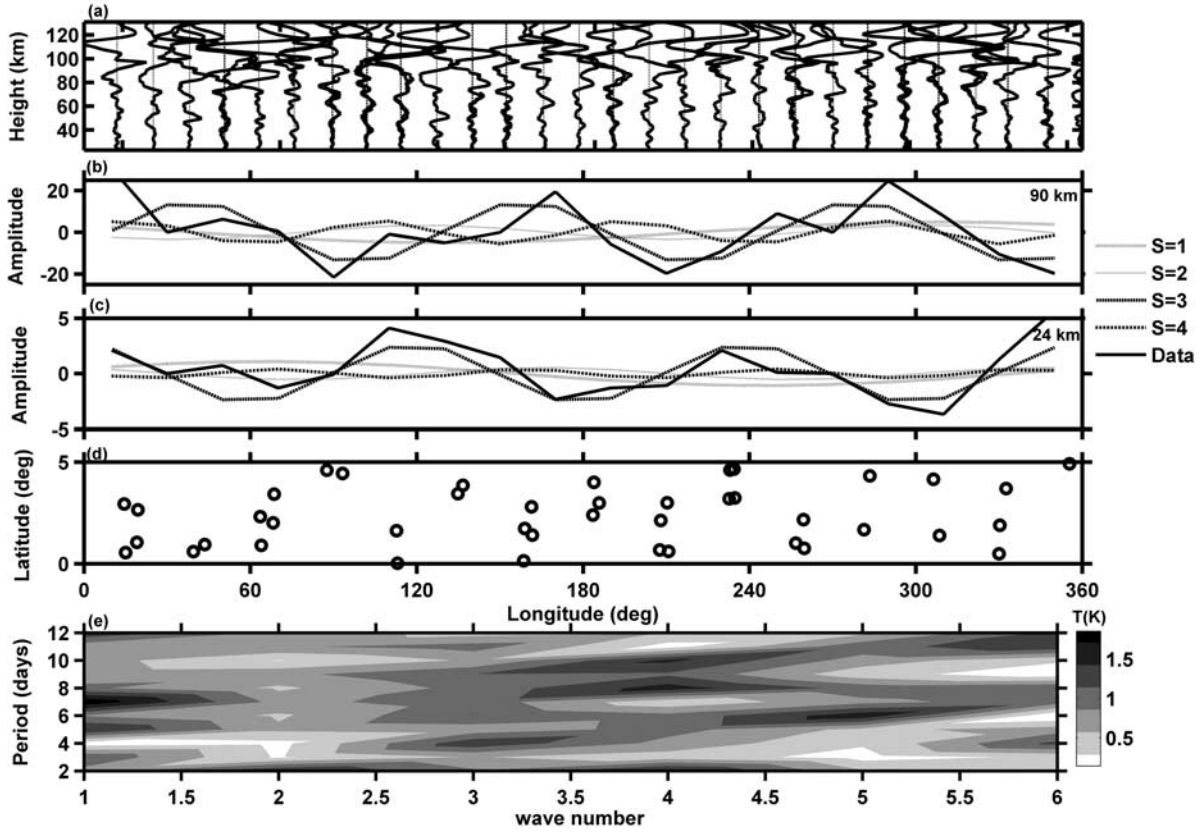

Figure 5. (a–d) Same as Figures 4a–4d but for 22 January 2005. (e) Same as Figure 4e but for January–February 2005.

cyclical in longitude with a finite time and has been applied earlier to SABER data by *Ern et al.* [2008]. FFT is performed on T' values from different longitudes corresponding to fixed latitude and the resultant Fourier coefficients are fed as inputs for further FFT analysis to obtain the frequency response. The wave number–frequency ($s - \omega$) spectrum is thus obtained. The data are then band-pass filtered in $s - \omega$ space in order to extract 5–8 day waves. The 30° longitude grid resolution of SABER allows the study of waves with $s \leq 6$. After band passing, reverse FFT is applied to the coefficients so that time series of perturbations can be constructed.

[15] As an example, profiles of temperature fluctuations (after removing the zonal mean as mentioned above) observed on 6 July 2004 are shown in Figure 4. Each profile is drawn at its corresponding longitude as indicated by a dotted vertical line. Note that most of the T' profiles were enhanced at higher altitudes as expected. The locations of individual SABER events are shown in Figure 4d. The temperature profiles in Figure 4a that occur at proximate locations are very similar, indicating the consistency of the SABER measurements. Figure 4b (and Figure 4c) shows the sinusoidal fit of wave numbers 1–4 (along longitude) along with the original temperature fluctuations T' at an altitude of 90 km (24 km) for symmetric wave components, showing the amplitude of temperature oscillations of approximately ~20 K (~3 K) and wave numbers 3–4. The antisymmetric component's amplitudes are too small; hence they are not considered for further analysis. Two dimensional spectral analyses have been performed on the July–August 2004 data in order to see the dominant wave periods and corresponding horizontal wave numbers, which are shown in Figure 4e. Note that during the entire period, the 6–8 day period is dominant with wave numbers 3–4, although small amplitudes with wave numbers 1–2 also coexist.

[16] Similar analysis has been performed for the observations made during January–February 2005. Profiles of temperature fluctuations observed on 22 January 2005 are shown in Figure 5. Again note that most of the T' profiles were enhanced at higher altitudes as expected. The locations of individual SABER events are shown in Figure 5d. The temperature profiles in Figure 5a that occur at proximate locations are also very similar. Figure 5b (and Figure 5c) shows the sinusoidal fit of wave numbers 1–4 (along longitude) at an altitude of 90 km (24 km) for symmetric wave components, showing the amplitude of temperature oscillations of approximately ~15 K (~3 K) and wave numbers 3–4 (3) structure. By performing such data processing over the long term, we can reveal the time evolution of the zonal wave propagation. Two dimensional spectral analyses have been performed on the January–February 2005 data and the results are shown in Figure 5e. Interestingly, note that during the entire period, the amplitude of the 5–8 day wave is small since the dominant period shifts to higher periods (8–10 days) with similar wave numbers 3–4.

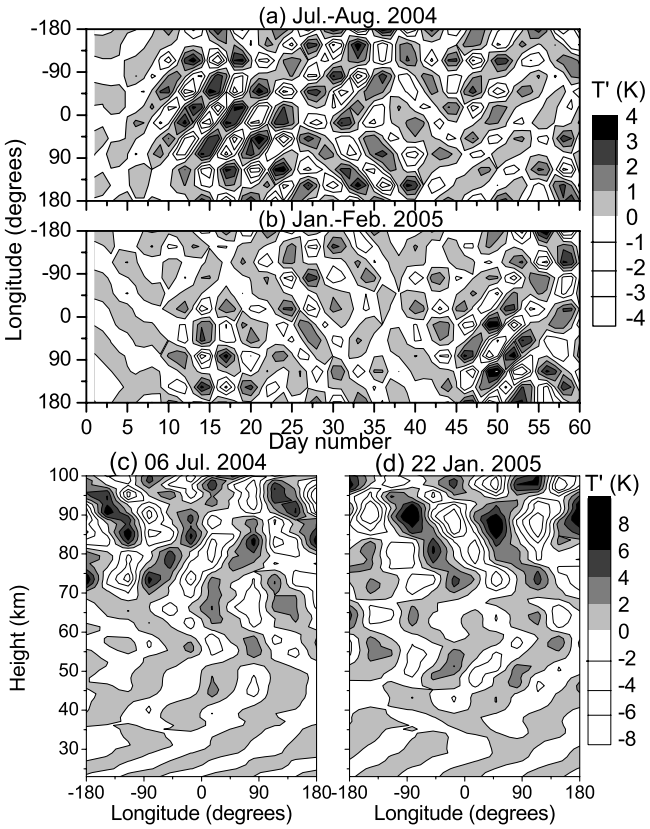

Figure 6. Time-longitude sections of filtered 5–8 day wave-related temperature fluctuations at 90 km altitude, constructed from wave numbers 3 and 4 for the observational period of (a) July–August 2004 and (b) January–February 2005. Examples showing the altitude-longitude sections of temperature fluctuations observed on (c) 6 July 2004 and (d) 22 January 2005. Positive and negative perturbations are shown in gray and white shades, respectively.

During January–February 2005, for the 5–8 day wave, wave number 1 dominates unlike during July–August 2004.

[17] Figure 6a shows the time-longitude section of the temperature extracted for the 5–8 day wave and wave numbers 3 and 4. The observations correspond to 90 km altitude and for the period of 1 July 2004 to 31 August 2004. This essentially demonstrates that the 5–8 day waves observed during July–August are global-scale waves. While an eastward phase progression is clearly seen most of the time, it is sometimes random and obscured, for example, at the last quarter of August. Patterns show mixed waves of wave numbers 3 and 4 dominating the entire period; however, some wave patterns along the longitude indicate the dominance of wave number 3. In contrast, time-longitude section of temperature variations at 90 km altitude during January–February 2005, presented in Figure 6b, shows westward phase progression except for the last quarter of February, where it is observed to be eastward. In general wave amplitude is about 4 K and at times reaches 6 K.

[18] In order to know the propagation characteristics of the observed 5–8 day waves, further analysis has been done to extract the height profile of the amplitude and the corresponding phase. Figures 6c and 6d show examples of the altitude-longitude sections of temperature variations of filtered 5–8 day period observed on 6 July 2004 and 22 January 2005, respectively. The increase in amplitude with altitude is consistent with that predicted for a conservative wave propagating upward. The amplitude of filtered (5–8 day) temperature is found to increase with height and become significantly large in the *E* region (100 km) with a value as high as 5.7 K. Note that, above 80 km altitude, the phase progression tilts westward and downward in both cases. However, in both cases phase progression shows eastward and upward below 50 km and westward and downward between 50 and 70 km. The estimated vertical wavelengths are in the range of 15–20 km. Note that we have also noticed 5–8 day Kelvin (eastward propagating) and Rossby (westward propagating) waves particularly during July–August 2004 between 90 and 100 km similar to that observed by *Pancheva et al.* [2008]. Since the observational period of July–August 2004 and January–February 2005 are in the eastward phase of quasi-biannual oscillation (QBO) [*Ratnam et al.*, 2006], it appears that the eastward phase of the QBO provides favorable conditions for the waves propagating westward. However, if the vertical phase speed is sufficiently larger than the background wind, eastward propagating waves can also propagate to higher heights (critical level interaction).

[19] Figures 7a and 7b show 5–8 day filtered SABER temperature corresponding to 100 km (thick dotted line) for the longitude belt of 60–90°E, radar echo occurrence (thick solid line), and Doppler velocity observed above 100 km (gray line) for July–August 2004 and January–February 2005, respectively. Temperature, echo occurrence, and Doppler velocity all show high values in July–August as compared to those in January–February. It is seen clearly that the amplitude of 5–8 day waves maximizes from day number 30 to 60. The amplitudes in temperature initially are higher than those of echo occurrence and Doppler velocity, but later amplitudes in the echo occurrence are higher than those of temperature and Doppler velocity. Initially, phase delay is observed in echo occurrence and Doppler velocity as compared to temperature. From day number 30–60, however, phase delay is observed in temperature and Doppler velocity as compared to echo occurrence. In January–February 2005, phase delay is observed in temperature as compared to occurrence and velocity. Phase delay is observed between temperature and echo occurrence, and the observed phase delay can be attributed to the long-period waves propagating upward as they grow in amplitude. It is to be noted that the generation and propagation of a wave should be seen differently. Not all waves generated below will propagate vertically. Moreover, propagation of a wave to higher heights would depend heavily on the background wind conditions. During generation, direct response can be seen in the fields of temperature and winds at higher heights, however, delay can be expected as the wave propagates upward. It is worth to mention that while the period of oscillation considered here is a band of 5–8 days, the dominant wave periods sometimes are found to be 6–7 days and 5–7 days. Hence the phase delay that we discussed above may not be true when period changes.

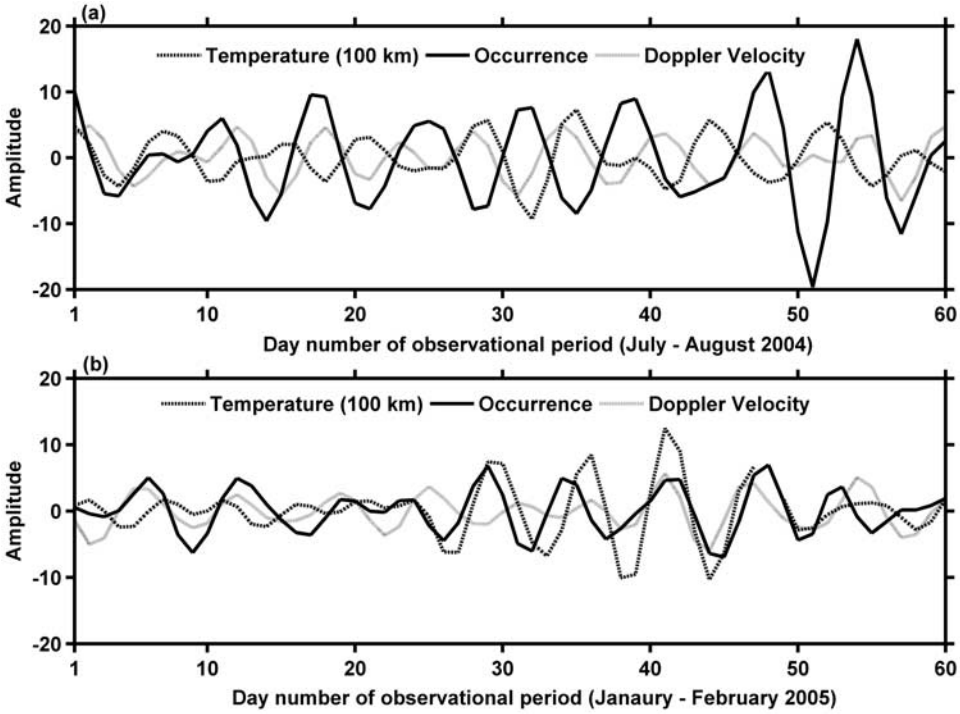

Figure 7. Wave amplitude observed in temperature at 100 km (thick dotted line), in the radar echo occurrence (thick solid line), and in the Doppler velocity (gray line) for (a) July–August 2004 and (b) January–February 2005.

However, our main interest is to examine to what extent the planetary wave signatures are present in all the parameters.

4. Discussion

[20] We have presented a clear signature of 5–8 day variability in the low-latitude FAI observations made using the Gadanki radar observations. These variabilities are found in the echo occurrence, in SNR, and also in the Doppler velocity observed above 100 km. The observed periodicities in FAI observations fall well within the band of well-known planetary-scale waves in the mesosphere and lower thermosphere [e.g., *Forbes*, 1994]. We have also observed contrasting features in July–August 2004 and January–February 2005, with maximum activity in the former and minimum activity in the latter case. Concurrent temperature observations made using SABER have also clearly shown the presence of 5–8 day variability with maximum activity in the former and minimum in the latter case, which are quite similar to those of FAI. The temperature variations have been characterized with zonal wave numbers of 3 and 4 and a vertical wavelength of 15 to 20 km. Further, height profile of these wave activities observed in temperature showed increasing amplitude with increasing height and also phase progressing downward, which are typical signatures for waves propagating from lower altitudes to higher altitudes and suggest that the planetary-scale waves observed during the observational period under consideration were of lower atmospheric origin. It may be mentioned that the planetary-scale variability at a given altitude can be studied using either temperature or wind. In fact, *Pancheva et al.* [2008] have observed similar planetary-scale variability in wind during June–December 2004, which falls in our observational period. Thus, the concurrent observations of FAI and temperature showing 5–8 days variability with similar seasonal dependence thus suggest the possible role of the 5–8 day wave in the variabilities of FAI parameters (echo occurrence, SNR, and velocity).

[21] As far as the observational evidence on planetary-scale variability in FAI is concerned, it is at present limited to midlatitudes [*Tsunoda et al.*, 1998; *Voiculescu et al.*, 1999, 2000]. It is interesting to note that while *Tsunoda et al.* [1998] have shown planetary-scale variability in QP echo occurrence, *Voiculescu et al.* [1999, 2000] have shown such variability in VHF radar echo occurrence itself. Here, in addition to echo occurrence, we have shown 5–8 day variability in SNR and velocity.

[22] To explain the midlatitude QP echo occurrence with the planetary-scale time period, *Tsunoda et al.* [1998] proposed that the planetary-scale wind-driven dynamo field could be generated if the *E* region conductivity is comparable to the *F* region and the vertical wavelength of the planetary-scale wave is greater than the thickness of the *E* region. These electric fields then could control the generation of FAI manifesting the planetary-scale variability in QP occurrence. On the other hand, planetary-scale variability in E_s was also shown by *Voiculescu et al.* [1999]. To account for the variabilities in E_s, *Shalimov et al.* [1999] used planetary-scale zonal wind shear in the meridional direction (i.e., the zonal wind changing with latitude) for ion convergence. This mechanism is similar to the well-known vertical wind shear mechanism, but the efficiency is more than that of the latter. Considering that midlatitude E_s and FAI occurrence are closely related [*Hussey et al.*, 1998; *Voiculescu et al.*, 1999], *Shalimov et al.* [1999]

argued that this mechanism would be able to account for the planetary-scale variability in FAI also. In this context, the proposal of *Tsunoda et al.* [1998] appears to be a weak proposition since it uses electric field with planetary-scale variation as a driving force, which cannot account for the observed planetary-scale E_s variability.

[23] In that regard, the proposal of *Shalimov et al.* [1999] looks quite appealing, but it was found later that it requires large-scale horizontal convergence of metallic ions [*Shalimov and Haldoupis*, 2002]. *Voiculescu and Ignat* [2003] performed a model study and suggested that linear superposition of tidal and planetary-scale wind fields can produce planetary-scale modulation in metallic ion densities, which would account for the planetary-scale variation in E_s occurrence. On the other hand, *Pancheva et al.* [2003] suggested that tides could be modulated by planetary-scale waves through nonlinear interaction resulting in large amplitude winds required for E_s formation to display planetary-scale variability. Since the mechanism requires the planetary-scale amplitudes to be large and the metallic ions need to have long lifetimes of the order of half the planetary-scale wave period under consideration [*Haldoupis et al.*, 2004], the mechanism proposed by *Pancheva et al.* [2003] appears to have an advantage over other proposals [*Shalimov et al.*, 1999; *Voiculescu and Ignat*, 2003]. *Pancheva et al.* [2003], however, mentioned that the possibility of E_s formation directly by planetary-scale winds cannot be ruled out.

[24] The above mechanism (meridional wind shear of zonal wind for E_s layer formation), however, when applied to low latitudes, becomes equivalent to that of vertical shear in zonal wind since the magnetic fields are nearly horizontal. If the meridional shear in zonal wind is considered to be more efficient in E_s layer formation than the vertical shear in zonal wind [*Shalimov et al.*, 1999], it is natural to argue that this mechanism would not work at low latitudes since both are identical for a near-horizontal magnetic field geometry. In fact, *Shalimov et al.* [1999] mentioned that this mechanism would not work at low latitudes. Thus the applicability of the mechanism that involves low-latitude E_s formation and the E_s becoming unstable to cause planetary-scale variability in FAI seems to be remote. In this context, the proposal given by *Tsunoda et al.* [1998] might be applicable for low latitudes. There are two observational aspects that work in support of the mechanism proposed by *Tsunoda et al.* [1998]. First, we have shown the Doppler velocities, which represent zonal electric field, to vary with planetary scale. *Tsunoda et al.* [1998] considered a varying electric field, and we have some signatures to support that idea. Second, *Patra et al.* [2005] earlier showed that low-latitude E_s and FAI have no close relation, unlike that of midlatitudes. Thus it appears to be very unlikely that the planetary-scale FAI variations are due to the unstable low-latitude E_s, which is modulated by the planetary-scale winds. Since we do not have simultaneous observations of E_s, it is only a conjecture. This aspect needs to be experimentally verified, a task to be left for future investigation.

5. Concluding Remarks

[25] We have shown for the first time that low-latitude FAI also have planetary-scale variation like those of the midlatitudes. We have also observed similar variations in concurrent temperature observations and found them to be upward propagating planetary-scale waves. Since the manifestations of wind characteristics (tides and gravity waves) have already been recognized in low-latitude FAI observations, the observations on planetary-scale variability reported here deserve attention. The present investigation, although preliminary at this stage, raises important questions on the role of planetary-scale waves in low-latitude plasma structuring and the generation of irregularities.

[26] **Acknowledgments.** The authors are grateful to the NARL technical staff for their dedicated efforts in making the observations reported here. One of the authors (D.V.P.) acknowledges NARL for offering a junior research fellowship. The authors gratefully acknowledge both the reviewers for their valuable comments and suggestions for the improvement of the paper. We thank Clia Goodwin for helping us in English editing.

[27] Amitava Bhattacharjee thanks John Sahr and another reviewer for their assistance in evaluating this paper.

References

Apostolov, E. M., D. Altadill, and L. Alberca (1995), Characteristics of quasi-2-day oscillations in the f_0F2 at northern middle latitudes, *J. Geophys. Res.*, *100*, 12,163, doi:10.1029/95JA00134.

Chau, J. L., and R. F. Woodman (1999), Low-latitude quasiperiodic echoes observed with the Piura VHF radar in the *E* region, *Geophys. Res. Lett.*, *26*, 2167, doi:10.1029/1999GL900488.

Chau, J. L., R. F. Woodman, and L. A. Flores (2002), Statistical characteristics of low latitude ionospheric field-aligned irregularities obtained with the Piura VHF radar, *Ann. Geophys.*, *20*, 1203.

Chen, P.-R. (1992), Two-day oscillation of the equatorial ionization anomaly, *J. Geophys. Res.*, *97*, 6343, doi:10.1029/91JA02445.

Choudhary, R. K., and K. K. Mahajan (1999), Tropical *E* region field aligned irregularities: Simultaneous observations of continuous and quasiperiodic echoes, *J. Geophys. Res.*, *104*, 2613, doi:10.1029/1998JA900012.

Choudhary, R. K., J.-P. St.-Maurice, L. M. Kagan, and K. K. Mahajan (2005), Quasi-periodic backscatters from the *E* region at Gadanki: Evidence for Kelvin-Helmholtz billows in the lower thermosphere?, *J. Geophys. Res.*, *110*, A08303, doi:10.1029/2004JA010987.

Ern, M., P. Preusse, M. Krebsbach, M. G. Mlynczak, and J. M. Russell III (2008), Equatorial wave analysis from SABER and ECMWF temperatures, *Atmos. Chem. Phys.*, *8*, 845.

Forbes, J. M. (1994), Tidal and planetary waves, in *The Upper Mesosphere and Lower Thermosphere: A Review of Experiment and Theory*, *Geophys. Monogr. Ser*, *87*, edited by R. M. Johnson and T. L. Killeen, p. 87, AGU, Washington, D. C.

Fraser, G. J. (1977), The 5-day wave and ionospheric absorption, *J. Atmos. Terr. Phys.*, *39*, 121, doi:10.1016/0021-9169(77)90053-8.

Haldoupis, C., and D. Pancheva (2002), Planetary waves and midlatitude sporadic *E* layers: Strong experimental evidence for a close relationship, *J. Geophys. Res.*, *107*(A6), 1078, doi:10.1029/2001JA000212.

Haldoupis, C., D. Pancheva, and N. J. Mitchell (2004), A study of tidal and planetary wave periodicities present in midlatitude sporadic *E* layers, *J. Geophys. Res.*, *109*, A02302, doi:10.1029/2003JA010253.

Hussey, G. C., K. Schlegel, and C. Haldoupis (1998), Simultaneous 50-MHz coherent backscatter and digital ionosonde observations in the midlatitude *E* region, *J. Geophys. Res.*, *103*, 6991, doi:10.1029/97JA03089.

Igarashi, K., and H. Kato (2001), The 2–16 day recurrence cycle of daily sporadic *E* activity and its relation to planetary wave activity observed with MF radar in spring and summer 1996, *Adv. Space Res.*, *27*, 1271, doi:10.1016/S0273-1177(01)00197-1.

Krishna Murthy, B. V., S. Ravindran, K. S. Viswanathan, K. S. V. Subbarao, A. K. Patra, and P. B. Rao (1998), Small-scale (~3 m) *E* region irregularities at and off the magnetic equator, *J. Geophys. Res.*, *103*, 20,761, doi:10.1029/98JA00928.

Lastovicka, J., V. Fiser, and D. Pancheva (1994), Long-term trends in planetary activity (2–15 days) at 80–100 km inferred from radio wave absorption, *J. Atmos. Terr. Phys.*, *56*, 893, doi:10.1016/0021-9169(94)90151-1.

Mertens, C. J., M. G. Mlynczak, M. López-Puertas, P. P. Wintersteiner, R. H. Picard, J. R. Winick, L. L. Gordley, and J. M. Russell III (2001), Retrieval of mesospheric and lower thermospheric kinetic temperature from measurements of CO_2 15 μm Earth limb emission under non-LTE conditions, *Geophys. Res. Lett.*, *28*, 1391, doi:10.1029/2000GL012189.

Pancheva, D., J. Laštovièka, and B. A. de la Morena (1991), Quasi-periodic fluctuations in ionospheric absorption in relation to planetary activity in the stratosphere, *J. Atmos. Terr. Phys.*, *53*, 1151, doi:10.1016/0021-9169(91)90065-F.

Pancheva, D., C. Haldoupis, C. E. Meek, A. H. Manson, and N. J. Mitchell (2003), Evidence of a role for modulated atmospheric tides in the dependence of sporadic *E* layers on planetary waves, *J. Geophys. Res.*, *108*(A5), 1176, doi:10.1029/2002JA009788.

Pancheva, D. V., P. J. Mukhtarov, N. J. Mitchell, D. C. Fritts, D. M. Riggin, H. Takahashi, P. P. Batista, B. R. Clemesha, S. Gurubaran, and G. Ramkumar (2008), Planetary wave coupling (5–6-day waves) in the low-latitude atmosphere-ionosphere system, *J. Atmos. Sol. Terr. Phys.*, *70*, 101, doi:10.1016/j.jastp.2007.10.003.

Patra, A. K., P. B. Rao, V. K. Anandan, A. R. Jain, and G. Viswanathan (2002), Evidence of intermediate layer characteristics in the Gadanki radar observations of the upper *E* region field-aligned irregularities, *Geophys. Res. Lett.*, *29*(14), 1696, doi:10.1029/2001GL013773.

Patra, A. K., S. Sripathi, V. Sivakumar, and P. B. Rao (2004), Statistical characteristics of VHF radar observations of low latitude *E* region irregularities over Gadanki, *J. Atmos. Sol. Terr.*, *66*, 1615, doi:10.1016/j.jastp.2004.07.032.

Patra, A. K., S. Sripathi, P. B. Rao, and K. S. V. Subbarao (2005), Simultaneous VHF radar backscatter and ionosonde observations of low-latitude *E* region, *Ann. Geophys.*, *23*, 773.

Patra, A. K., S. Sripathi, P. B. Rao, and R. K. Choudhary (2006), Gadanki radar observations of daytime *E* region echoes and structures extending down to 87 km, *Ann. Geophys.*, *24*, 1861.

Patra, A. K., T. Yokoyama, M. Yamamoto, T. Nakamura, T. Tsuda, and S. Fukao (2007), Lower *E* region field-aligned irregularities studied using the Equatorial Atmosphere Radar and meteor radar in Indonesia, *J. Geophys. Res.*, *112*, A01301, doi:10.1029/2006JA011825.

Rao, P. B., A. R. Jain, K. Kishore, P. Balamuralidhar, S. H. Damle, and G. Viswanathan (1995), Indian MST radar: 1. System description and sample vector wind measurements in ST mode, *Radio Sci.*, *30*, 1125, doi:10.1029/95RS00787.

Ratnam, M. V., T. Tsuda, T. Kozu, and S. Mori (2006), Long-term behavior of the Kelvin waves revealed by CHAMP/GPS RO measurements and their effects on the tropopause structure, *Ann. Geophys.*, *24*, 1355.

Shalimov, S., and C. Haldoupis (2002), A model of midlatitude *E* region plasma convergence inside a planetary wave cyclonic vortex, *Ann. Geophys.*, *20*, 1193.

Shalimov, S., C. Haldoupis, M. Voiculescu, and K. Schlegel (1999), Midlatitude *E* region plasma accumulation driven by planetary wave horizontal wind shears, *J. Geophys. Res.*, *104*, 28,207, doi:10.1029/1999JA900316.

Sripathi, S., A. K. Patra, V. Sivakumar, and P. B. Rao (2003), Shear instability as a source of the daytime quasi-periodic radar echoes observed by the Gadanki VHF radar, *Geophys. Res. Lett.*, *30*(22), 2149, doi:10.1029/2003GL017544.

Tsunoda, R. T., M. Yamamoto, K. Igarashi, K. Hocke, and S. Fukao (1998), Quasi-periodic radar echoes from midlatitude sporadic *E* and role of the 5-day planetary wave, *Geophys. Res. Lett.*, *25*, 951, doi:10.1029/98GL00663.

Venkateswara Rao, N., A. K. Patra, and S. V. B. Rao (2008), Some new aspects of low-latitude *E*-region QP echoes revealed by Gadanki radar: Are they due to Kelvin-Helmholtz instability or gravity waves?, *J. Geophys. Res.*, *113*, A03309, doi:10.1029/2007JA012574.

Voiculescu, M., and M. Ignat (2003), Vertical motion of ionization induced by the linear interaction of tides and planetary waves, *Ann. Geophys.*, *21*, 1521.

Voiculescu, M., C. Haldoupis, and K. Schlegel (1999), Evidence for planetary wave effects on midlatitude backscatter and sporadic *E* layer occurrence, *Geophys. Res. Lett.*, *26*, 1105, doi:10.1029/1999GL900172.

Voiculescu, M., C. Haldoupis, D. Pancheva, M. Igant, K. Schlegel, and S. Shalimov (2000), More evidence for a planetary wave link with midlatitude *E* region coherent backscatter and sporadic *E* layers, *Ann. Geophys.*, *18*, 1182, doi:10.1007/s00585-000-1182-8.

Woodman, R. F., J. L. Chau, F. Aquino, R. R. Rodriguez, and L. A. Flores (1999), Low-latitude field-aligned irregularities observed in the *E* region with the Piura VHF radar: First results, *Radio Sci.*, *34*, 983, doi:10.1029/1999RS900027.

Wu, D. L., P. B. Hays, and W. R. Skinner (1994), Observations of the 5-day wave in the mesosphere and lower thermosphere, *Geophys. Res. Lett.*, *21*, 2733, doi:10.1029/94GL02660.

Xu, J., H.-L. Liu, W. Yuan, A. K. Smith, R. G. Roble, C. J. Mertens, J. M. Russell III, and M. G. Mlynczak (2007), Mesopause structure from Thermosphere, Ionosphere, Mesosphere, Energetics, and Dynamics (TIMED)/Sounding of the Atmosphere Using Broadband Emission Radiometry (SABER) observations, *J. Geophys. Res.*, *112*, D09102, doi:10.1029/2006JD007711.

Yamamoto, M., S. Fukao, R. F. Woodman, T. Ogawa, T. Tsuda, and S. Kato (1991), Midlatitude *E* region field-aligned irregularities observed with the MU radar, *J. Geophys. Res.*, *96*, 15,943, doi:10.1029/91JA01321.

A. K. Patra, D. V. Phanikumar, and M. V. Ratnam, National Atmospheric Research Laboratory, Gadanki, 517112, India. (akpatra@narl.gov.in)

S. Sripathi, Indian Institute of Geomagnetism, Navi Mumbai, 410218, India.